

# Combination of the LEP II $f\bar{f}$ Results

## LEPEWWG $f\bar{f}$ Subgroup

Members :

C. Geweniger, C. Goy, M-N Minard  
M. Elsing, J. Holt, W. Liebig, A. Olshevski, P. Renton  
S. Blyth, D. Bourilkov, S. Riemann, S. Wynhoff  
F. Fiedler, M. Kobel, S. Marcellini, K. Sachs, P. Ward

### Abstract

Preliminary combinations of measurements of the 4 LEP collaborations of the process  $e^+e^- \rightarrow f\bar{f}$  at LEP II are presented. Cross-sections and forward-backward asymmetry measurements are combined for the full LEP II data set. A first combination of differential cross-sections  $\frac{d\sigma}{d\cos\theta}$  for muon-pair and tau-pair final states is presented. Measurements of the production of heavy flavours are also combined. The combined results are interpreted in terms of contact interactions, exchange of  $Z'$  bosons, and contours of the S-Matrix parameters  $j_{b,c}^{\text{tot}}$  and  $j_{b,c}^{\text{fb}}$  that describe  $\gamma - Z$  interference in heavy-flavour production in fermion-pair production are derived.

# 1 Introduction

Since the start of the LEP II program LEP has delivered collisions at energies from  $\sim 130$  GeV to  $\sim 209$  GeV. The 4 LEP experiments have made measurements on the  $e^+e^- \rightarrow f\bar{f}$  process over this range of energies, and a preliminary combination of these data are discussed in this note.

In the years 1995 through 1999 LEP delivered luminosity at a number of distinct centre-of-mass energy points. In 2000 most of the luminosity was delivered close to 2 distinct energies, but there was also a significant fraction of the luminosity delivered in, more-or-less, a continuum of energies. To facilitate the combination of the data, the 4 LEP experiments all divided the data they collected in 2000 into two energy bins: from 202.5 to 205.5 GeV; and 205.5 GeV and above. For the combination presented here, only data taken up to the end of June 2000 are considered. The nominal and actual centre of mass energies to which the LEP data have been averaged for each year are given in Table 1.

A number of measurements on the process  $e^+e^- \rightarrow f\bar{f}$  exist and have been combined. The preliminary averages of cross-section and forward-backward asymmetry measurements are discussed in Section 2. The results presented in this section update those presented in [1] and [2]. In Section 3 a preliminary average of the differential cross-sections measurements,  $\frac{d\sigma}{d\cos\theta}$ , for the channels  $e^+e^- \rightarrow \mu^+\mu^-$  and  $e^+e^- \rightarrow \tau^+\tau^-$  is discussed. This is the first attempt to combine these data. In Section 4 an update of the combinations of heavy flavour results  $R_b$ ,  $R_c$ ,  $A_{FB}^b$  and  $A_{FB}^c$  from LEP II is presented. Complete results of the combinations are available on the web page [3].

In Section 5 the combined results are interpreted in terms of contact interactions, the exchange of  $Z'$  bosons, and contours of the S-Matrix parameters  $j_{b,c}^{\text{tot}}$  and  $j_{b,c}^{\text{fb}}$ , that describe  $\gamma - Z$  interference, are derived.

The results are summarised in section 6, and future plans for the combination of LEP II  $f\bar{f}$  data are discussed.

## 2 Averages for Cross-sections and Asymmetries

In this section the results of the preliminary combination of cross-sections and asymmetries are given. The individual experiments' analyses of cross-sections and forward-backward asymmetries are discussed in [4]. Cross-section results are combined for the  $e^+e^- \rightarrow q\bar{q}$ ,  $e^+e^- \rightarrow \mu^+\mu^-$  and  $e^+e^- \rightarrow \tau^+\tau^-$  channels, forward-backward asymmetry measurements are combined for the  $\mu^+\mu^-$  and  $\tau^+\tau^-$  final states. The averages are made for the samples of events with high  $\sqrt{s'}$ . The combination followed the procedure described in detail in [2], and is only briefly reviewed here.

At LEP2 energies radiative processes in  $e^+e^- \rightarrow f\bar{f}$  are very important, and in particular interference between initial- and final-state radiation leads to ambiguities in the definition of the reduced centre-of-mass energy  $\sqrt{s'}$ . Different experiments have adopted different procedures in the experimental estimation and theoretical definition of  $s'$ . Before averaging the results, it is necessary to choose a common definition of the  $f\bar{f}$  signal and correct the results of the four experiments to this common definition. In [2], two different definitions were used:

- **Definition 1:**  $\sqrt{s'}$  is taken to be the mass of the  $s$ -channel propagator, with the  $f\bar{f}$  signal being defined by the cut  $\sqrt{s'/s} > 0.85$ . ISR-FSR photon interference is subtracted to render the propagator mass unambiguous.
- **Definition 2:** For dilepton events,  $\sqrt{s'}$  is taken to be the bare invariant mass of the outgoing dilepton pair. For hadronic events, it is taken to be the mass of the  $s$ -channel

Year	Nominal Energy GeV	Actual Energy GeV	Luminosity $\text{pb}^{-1}$
1995	130	130.2	$\sim 3$
	136	136.2	$\sim 3$
	133*	133.2	$\sim 6$
1996	161	161.3	$\sim 10$
	172	172.1	$\sim 10$
	167*	166.6	$\sim 20$
1997	130	130.2	$\sim 2$
	136	136.2	$\sim 2$
	183	182.7	$\sim 50$
1998	189	188.6	$\sim 170$
1999	192	191.6	$\sim 30$
	196	195.5	$\sim 80$
	200	199.5	$\sim 80$
	202	201.6	$\sim 40$
2000	205	204.9	$\sim 60$
	207	206.7	$\sim 30$
	206*	205.5	$\sim 90$

Table 1: *The nominal and actual centre-of-mass energies for data collected during LEP II operation in each year. The approximate average luminosity analysed per experiment at each energy is also shown. Values marked with a \* are average energies for 1995, 1996 and 2000 used for heavy flavour results. The data taken at nominal energies of 130 and 136 in 1995 and 1997 are combined by most experiments.*

propagator. In both cases, ISR-FSR photon interference is included and the signal is defined by the cut  $\sqrt{s'/s} > 0.85$ . When calculating the contribution to the hadronic cross-section due to ISR-FSR interference, since the propagator mass is ill-defined, it is replaced by the bare  $q\bar{q}$  mass.

Before they are averaged, the measurements from each experiment are corrected to the common choice of signal definition using an additive correction calculated using the semi-analytic program ZFITTER v6.10 [5]. As a result of this, the shifts in the combined results between the two definitions are identical to the difference in the Standard Model (SM) values between the different definitions. In this note we present results according to definition 1, and give the shifts necessary to obtain definition 2. The theoretical uncertainties associated with the corrections were obtained by comparing ZFITTER, TOPAZ0 v4.4 [6] and the Monte Carlo generator KK v4.02 [7]. The uncertainties are 0.2% for the hadronic cross-sections, 0.7% for dilepton cross-sections and 0.003 for the leptonic asymmetries [2]. Results are presented inside the full  $4\pi$  angular acceptance. Events containing additional fermion pairs from radiative processes are considered to be signal, providing that the primary pair passes the cut on  $\sqrt{s'/s}$  and that the secondary pair has a mass below  $70 \text{ GeV}/c^2$ .

Input data were supplied by the experiments in the format described in [2]. These consist of measurements of the cross-sections for  $q\bar{q}$ ,  $\mu^+\mu^-$  and  $\tau^+\tau^-$ , and the asymmetries for the lepton-pairs, together with the errors broken down into five subcomponents according to whether or not they are correlated between channels and experiments, as follows:

- 1) The statistical uncertainty plus uncorrelated systematic uncertainties, combined in quadrature.
- 2) The systematic uncertainty for the final state X which is fully correlated between energy points for that experiment.
- 3) The systematic uncertainty for experiment Y which is fully correlated between different final states for this energy point.
- 4) The systematic uncertainty for the final state X which is fully correlated between energy points and between different experiments.
- 5) The systematic uncertainty which is fully correlated between energy points and between different experiments for all final states.

The theoretical predictions, calculated using ZFITTER [5], were also given, in order to correct experimental measurements to the common signal definition. As discussed in [1], in cases where fewer than 100 events were observed, the expected statistical errors on the asymmetry measurements were used.

The averages were performed using a  $\chi^2$  minimisation technique. The data were split into 3 sets: data taken at energies from 130–189 GeV, data taken during 1999, and data taken in 2000. Averages were performed separately for each of these data sets. This procedure ignores correlations between the 1999 and 2000 data and also correlations between these two sets of data and the data taken at 130–189 GeV. This procedure was adopted because the 1999 and 2000 data are still preliminary, whereas the 130–189 GeV averages are based on published data. Inclusion of these correlations would have only a small effect on the results.

For each subset of data the error matrix  $E$  on these measurements is constructed, such that its element  $i, j$  is given by

$$E_{ij} = \sum_{k=1}^5 C_{ij}^k \sigma_i^k \sigma_j^k,$$

where the sum extends over the five error contributions described above.  $\sigma_i^k$  represents the uncertainty on measurement  $i$  due to error source  $k$  ( $1 \leq k \leq 5$ ). The factor  $C_{ij}^k$  is equal to 1 if error  $k$  correlates measurements  $i$  and  $j$  and equals zero if it does not. The  $\chi^2$  which must be minimised to obtain the averages is then

$$\chi^2 = (\mathbf{V} - \mathbf{A})^T E^{-1} (\mathbf{V} - \mathbf{A}),$$

where  $\mathbf{V}$  is a vector containing the corrected input measurements, and  $\mathbf{A}$  is a vector containing the desired averages corresponding to each of these measurements. This  $\chi^2$  has been minimised both analytically and using a numerical minimisation program. The results are identical.

Table 2 shows the preliminary combined results for the 1999 data corresponding to the signal definition 1 and the difference in the results if definition 2 is used. The results for the averages of the 130–189 GeV data are identical to those given in [1]. Results for the more preliminary data taken during 2000 are not given in numerical form but are shown in Figures 1 and 2 which show the LEP averaged cross-sections and asymmetries (based on definition 1), respectively, as a function of the centre-of-mass energy, together with the SM predictions.

The  $\chi^2$  per degree of freedom for the average of the 1999 data is 52.5/60. The correlations are rather small, with the largest components at any given pair of energies being between the hadronic cross-sections. The correlations between the averaged hadronic cross-sections are given in Table 3. The other off-diagonal terms in the correlation matrix are smaller than 10%. The full correlation matrix is given at [3].

There is good agreement between the SM expectations and the measurements of the individual experiments and the combined averages. The cross-sections for hadronic final states at most of the energy points are somewhat above the SM expectations. Taking into account the correlations between the data points and also assigning an error of  $\pm 0.5\%$  [8] on the absolute SM predictions, the difference of the cross-section from the SM expectations averaged over all energies is approximately a 2.5 standard deviation excess. It is concluded that there is no significant evidence in the results of the combinations for physics beyond the SM in the process  $e^+e^- \rightarrow f\bar{f}$ .

### 3 Averages for Differential Cross-sections

The LEP experiments have measured the differential cross-section,  $\frac{d\sigma}{d\cos\theta}$ , for the  $e^+e^- \rightarrow \mu^+\mu^-$  and  $e^+e^- \rightarrow \tau^+\tau^-$  channels. This section discusses a procedure to combine these measurements and presents preliminary results.

For several LEP energies the expected numbers of events in the backward region of  $\cos\theta$ ,  $\cos\theta < -0.8$ , is small. Statistical fluctuations can easily lead to no observed events in this region for any single experiment. Simply averaging the results using a  $\chi^2$  minimisation, or equivalent method, taking the statistical error computed from the square root of the number of observed events is expected to lead to a significant bias towards low cross-sections in the averaged results. A proper statistical treatment would compute the expected numbers of events for each experiment for an average cross-section, then use a likelihood fit to the actual number of observed events in the different experiments. Using a Monte Carlo simulation it was found that a  $\chi^2$  fit to the measured differential cross-sections, using the expected error on the differential cross-sections, computed from the expected cross-sections and the expected numbers of events in each experiment, provided a very good approximation to the exact likelihood method. This is discussed in more detail in Appendix A. The method is used to combine data from all bins at all energies, not just those with low statistics in the most backward bins.

$\sqrt{s}$ (GeV)	Quantity	Average value	SM prediction	$\Delta$
192	$\sigma(q\bar{q})$ [pb]	$22.292\pm 0.514$	21.237	-0.098
	$\sigma(\mu^+\mu^-)$ [pb]	$2.941\pm 0.175$	3.097	-0.127
	$\sigma(\tau^+\tau^-)$ [pb]	$2.863\pm 0.216$	3.097	-0.047
	$A_{\text{FB}}(\mu^+\mu^-)$	$0.540\pm 0.052$	0.566	0.019
	$A_{\text{FB}}(\tau^+\tau^-)$	$0.610\pm 0.071$	0.566	0.019
196	$\sigma(q\bar{q})$ [pb]	$20.730\pm 0.330$	20.127	-0.094
	$\sigma(\mu^+\mu^-)$ [pb]	$2.965\pm 0.106$	2.962	-0.123
	$\sigma(\tau^+\tau^-)$ [pb]	$3.015\pm 0.139$	2.962	-0.045
	$A_{\text{FB}}(\mu^+\mu^-)$	$0.579\pm 0.031$	0.562	0.019
	$A_{\text{FB}}(\tau^+\tau^-)$	$0.489\pm 0.045$	0.562	0.019
200	$\sigma(q\bar{q})$ [pb]	$19.376\pm 0.306$	19.085	-0.090
	$\sigma(\mu^+\mu^-)$ [pb]	$3.038\pm 0.104$	2.834	-0.118
	$\sigma(\tau^+\tau^-)$ [pb]	$2.995\pm 0.135$	2.833	-0.044
	$A_{\text{FB}}(\mu^+\mu^-)$	$0.518\pm 0.031$	0.558	0.019
	$A_{\text{FB}}(\tau^+\tau^-)$	$0.546\pm 0.043$	0.558	0.019
202	$\sigma(q\bar{q})$ [pb]	$19.291\pm 0.425$	18.572	-0.088
	$\sigma(\mu^+\mu^-)$ [pb]	$2.621\pm 0.139$	2.770	-0.116
	$\sigma(\tau^+\tau^-)$ [pb]	$2.806\pm 0.183$	2.769	-0.043
	$A_{\text{FB}}(\mu^+\mu^-)$	$0.543\pm 0.048$	0.556	0.020
	$A_{\text{FB}}(\tau^+\tau^-)$	$0.580\pm 0.060$	0.556	0.019

Table 2: Preliminary combined LEP results for  $e^+e^- \rightarrow f\bar{f}$ . All the results correspond to the signal definition 1. The Standard Model predictions are from ZFITTER [5]. The difference,  $\Delta$ , in the averages for the measurements for definition 2 relative to definition 1 are given in the final column. The quoted uncertainties do not include the theoretical uncertainties on the corrections discussed in the text.

$\sqrt{s}$ (GeV)	Correlations			
	192	196	200	202
192	1.000	0.099	0.113	0.080
196	0.099	1.000	0.159	0.114
200	0.113	0.159	1.000	0.128
202	0.080	0.114	0.128	1.000

Table 3: The correlation matrix of the averaged hadronic cross-section results.

preliminary

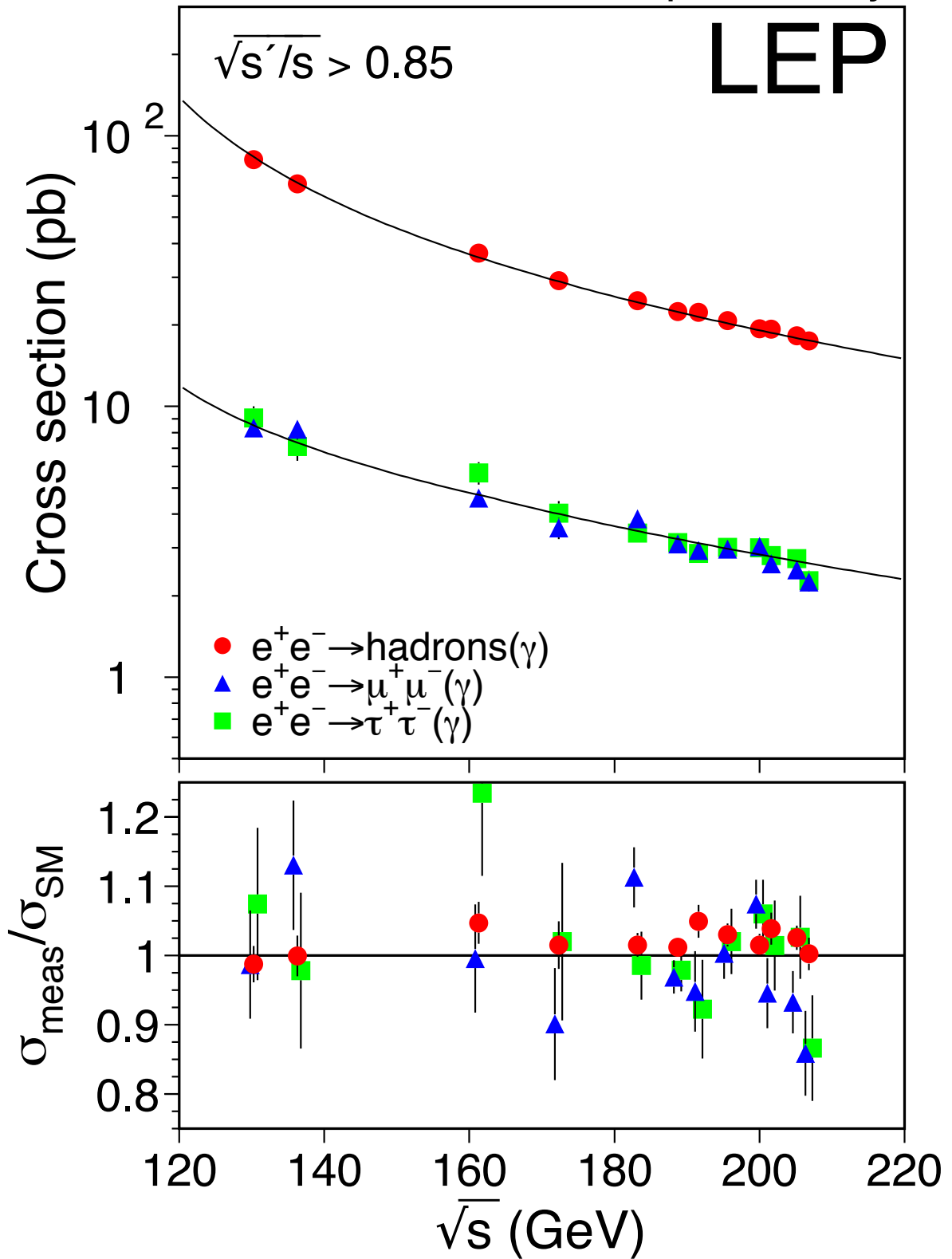


Figure 1: Preliminary combined LEP results on the cross-sections for  $q\bar{q}$ ,  $\mu^+\mu^-$  and  $\tau^+\tau^-$  final states, as a function of centre-of-mass energy. The values at 130–189 GeV are taken from [1]. The expectations of the SM, computed with ZFITTER [5], are shown as curves. The lower plot shows the ratio of the data divided by the SM.

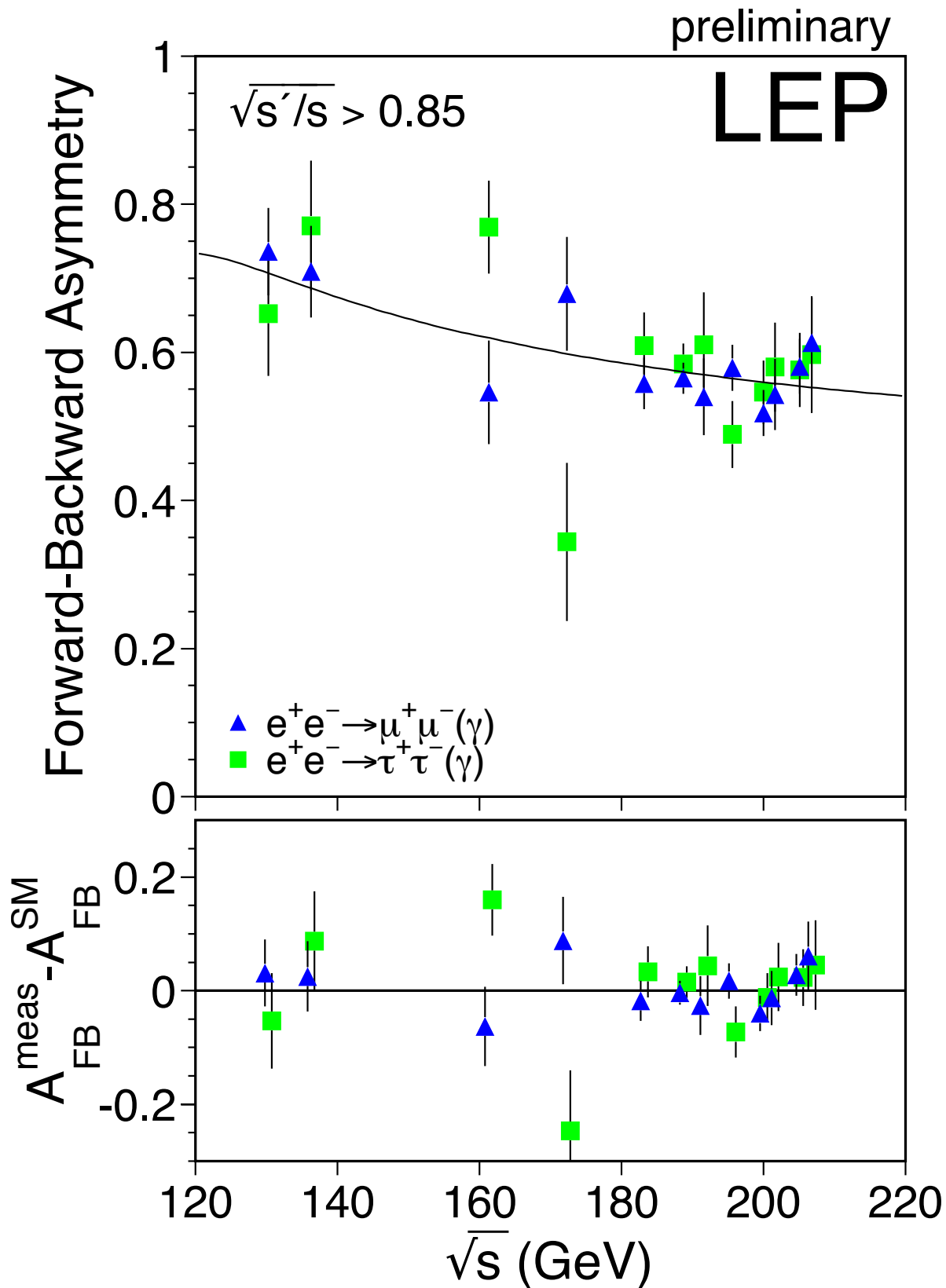


Figure 2: Preliminary combined LEP results on the forward-backward asymmetry for  $\mu^+\mu^-$  and  $\tau^+\tau^-$  final states as a function of centre-of-mass energy. The values at 130–189 GeV are taken from [1]. The expectations of the SM computed with ZFITTER [5], are shown as curves. The lower plot shows differences between the data and the SM.

$\sqrt{s}(\text{GeV})$	ALEPH	DELPHI	L3	OPAL
183	-	F	-	F
189	P	F	F	F
192-202	P	P	-	P

Table 4: *Differential cross-section data provided by the LEP collaborations for combination at different centre-of-mass energies. Data indicated with F are final, published data. Data marked with P are preliminary. Data marked with a - were not supplied for combination.*

The combination included data from 183 to 202 GeV, but not all experiments provided data at all energies. The data received are summarised in Table 4. The average is only made for samples of events with  $\sqrt{s'/s} > 0.85$ .

Data were binned in 10 bins of  $\cos\theta$ . The scattering angle,  $\theta$ , is the angle of the negative lepton with respect to the incoming electron direction in the lab coordinate system. The outer acceptances of the most forward and most backward bins for which the four experiments have presented their data are different. The acceptances of the experiments' results for the most extreme bins are given in Table 5. All other bins have identical acceptance in the four experiments.

As in the averages of the cross-sections and asymmetries the inputs of the experiments correspond to slightly different signal definitions. These are corrected to a common definition, in which  $\sqrt{s'}$  is taken to be the mass of the  $s$ -channel propagator, with the  $\bar{f}\bar{f}$  signal being defined by the cut  $\sqrt{s'/s} > 0.85$ . ISR-FSR photon interference is subtracted to render the propagator mass unambiguous. This corresponds to definition 1 of Section 2. The corrections applied include a correction from the different experimental acceptances in  $\cos\theta$  to a common signal acceptance of  $|\cos\theta| = 1.00$  for the most backward and most forward bins.

The correction is applied in the following way:

$$\left. \frac{d\sigma}{d\cos\theta} \right|_{\text{common}}^{\text{Measured}} = \left. \frac{d\sigma}{d\cos\theta} \right|_{\text{experiment}}^{\text{Measured}} + \left( \left. \frac{d\sigma}{d\cos\theta} \right|_{\text{common}}^{\text{SM}} - \left. \frac{d\sigma}{d\cos\theta} \right|_{\text{experiment}}^{\text{SM}} \right)$$

The corrected data are then averaged. Systematic errors were taken into account. Uncorrelated systematic errors are added in quadrature to the statistical errors. In addition systematic error arising from uncertainties on the overall normalisation were considered. These are correlated between bins, and can be correlated between different energies, channels and experiments. The same five classes of error were considered as in Section 2 for the averages of the total cross-sections.

Two separate averages were performed one for 183 and 189 GeV data and one for 192–202 GeV data. The results of the averages are shown in Figures 3, 4 and 5. Figure 3 also shows the inputs for the  $e^+e^- \rightarrow \mu^+\mu^-$  channel at 189 GeV. The correlations between bins in the average are less than 2% of the total error on the averages in each bin. Overall the agreement between the averaged data and the predictions is good, with a  $\chi^2$  of 114 for 120 degrees of freedom. At 202 GeV the cross-section in the most backward bin,  $-1.00 < \cos\theta < 0.8$ , for both muon and tau final states is above the predictions. For the muons the excess in data corresponds to 3.3 standard deviations. For the taus the excess is 2.3 standard deviations, however, for this measurement the individual experiments are somewhat inconsistent, having a chi-squared with respect to the average of 10.5 for 2 degrees of freedom.

The sources of systematic error considered above only affect the normalisation of the distribution. There could also be errors which affect the shape of the distribution, for example an

Experiment	$\cos \theta_{min}$	$\cos \theta_{max}$
ALEPH	-0.95	0.95
DELPHI ( $e^+e^- \rightarrow \mu^+\mu^-$ 183)	-0.94	0.94
DELPHI ( $e^+e^- \rightarrow \mu^+\mu^-$ 189 – 202)	-0.97	0.97
DELPHI ( $e^+e^- \rightarrow \tau^+\tau^-$ )	-0.96	0.96
L3	-0.90	0.90
OPAL	-1.00	1.00
Average	-1.00	1.00

Table 5: *The acceptances for which experimental data are presented and the acceptance for the LEP average. For DELPHI the acceptance is shown for the different channels and for the muons for different centre of mass energies. For all other experiments the acceptance is the same for muon and tau-lepton channels and for all energies provided.*

error arising from corrections due to the interference between initial and final state radiation. Figure 6 shows the difference in the predicted cross-sections with and without interference. For the 183 and 189 GeV data a second fit was performed taking 1/4 of this difference as an error to be applied to each bin. A contribution to the off diagonal elements of the error matrix was formed from the product of errors on each piece of data. Thus for example the contribution to the error matrix between the first and second most backward bins for muons at 189 GeV is positive, but the contribution to the error matrix between the most forward and most backward bins is negative. Thus the correlation coefficients between errors which change the shape of the distribution can be either positive or negative, those which are considered to affect the overall normalisation are all positive. The inclusion of the additional uncertainties did not affect the averages and did not significantly affect the final error. The absolute size of the correlations between the averages remained below 2% of the total errors.

## 4 Averages for Heavy Flavour Measurements

This section presents a combination of both published [9] and preliminary [10] measurements of the ratios\*  $R_b$  and  $R_c$  and the forward-backward asymmetries,  $A_{FB}^b$  and  $A_{FB}^c$ , from the LEP collaborations at centre-of-mass energies in the range of 130 to 209 GeV. Full details concerning the combination procedure can be found in [11]. For the purpose of averaging, a common signal definition has been defined for all the measurements, requiring:

- an effective centre-of-mass energy  $\sqrt{s'} > 0.85\sqrt{s}$
- the inclusion of ISR and FSR photon interference contribution and
- extrapolation to full angular acceptance.

When necessary, the measurements have been corrected to the common signal definition using ZFITTER [12] predictions.

The averaging procedure follows the method described in [13]. In particular, the dependencies of each of the measurements on the other parameters are explicitly accounted for. Systematic errors are divided into 3 categories: internal errors, errors correlated between the measurements of each experiment, and errors common to all experiments. Table 6 summarises the inputs that have been combined, yielding the results presented in Table 7 and Figures 7 and 8. A list of the error contributions from the combination at 189 GeV is shown in Table 8. The results are consistent with the Standard Model predictions of ZFITTER.

---

\*Unlike at LEP I,  $R_q$  is defined as  $\frac{\sigma_{q\bar{q}}}{\sigma_{had}}$ .

## $\mu\mu$ 189 GeV Preliminary

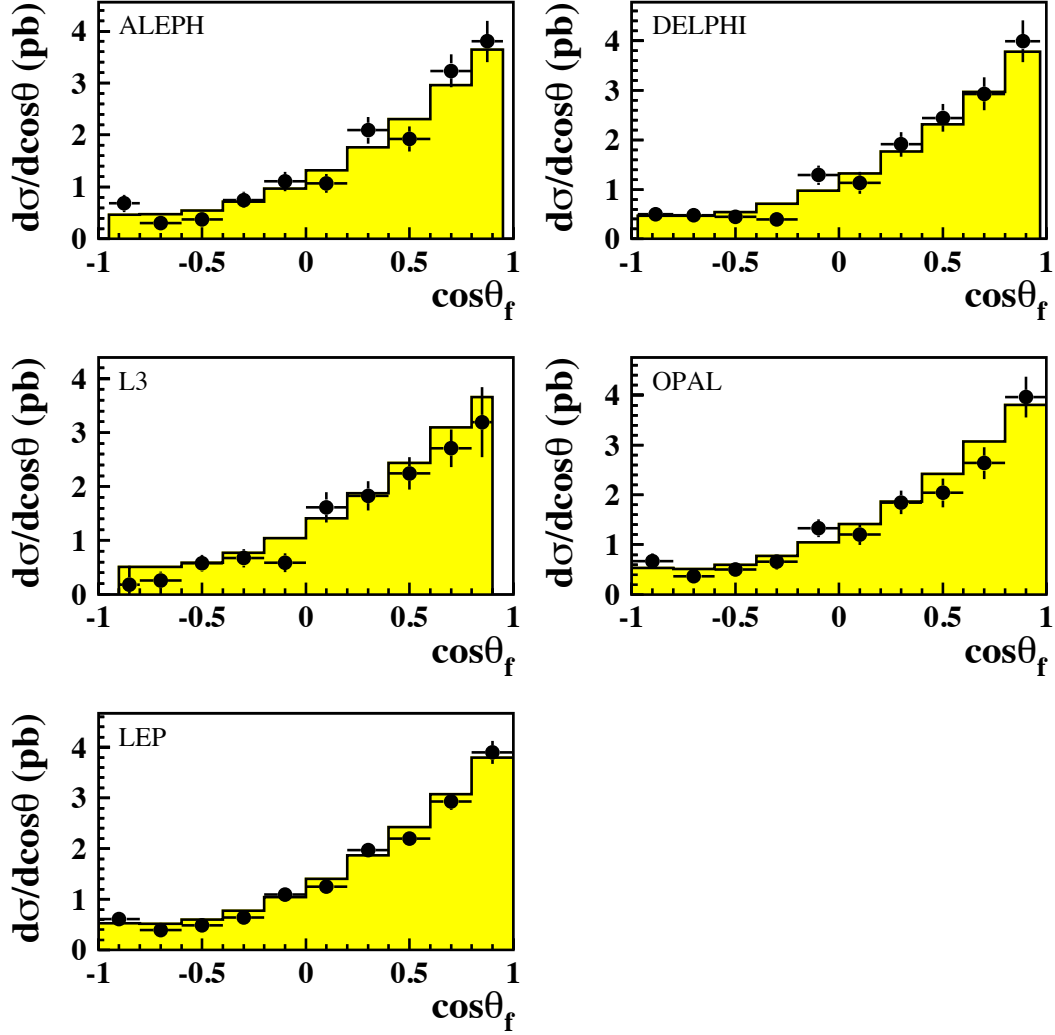


Figure 3: *Input differential cross-sections for  $e^+e^- \rightarrow \mu^+\mu^-$  at 189 GeV for ALEPH, DELPHI, L3 and OPAL, and the LEP average. The SM predictions, shown as solid histograms, are computed with ZFITTER.*

### Preliminary LEP Averaged $d\sigma/d\cos\theta$ ( $\mu\mu$ )

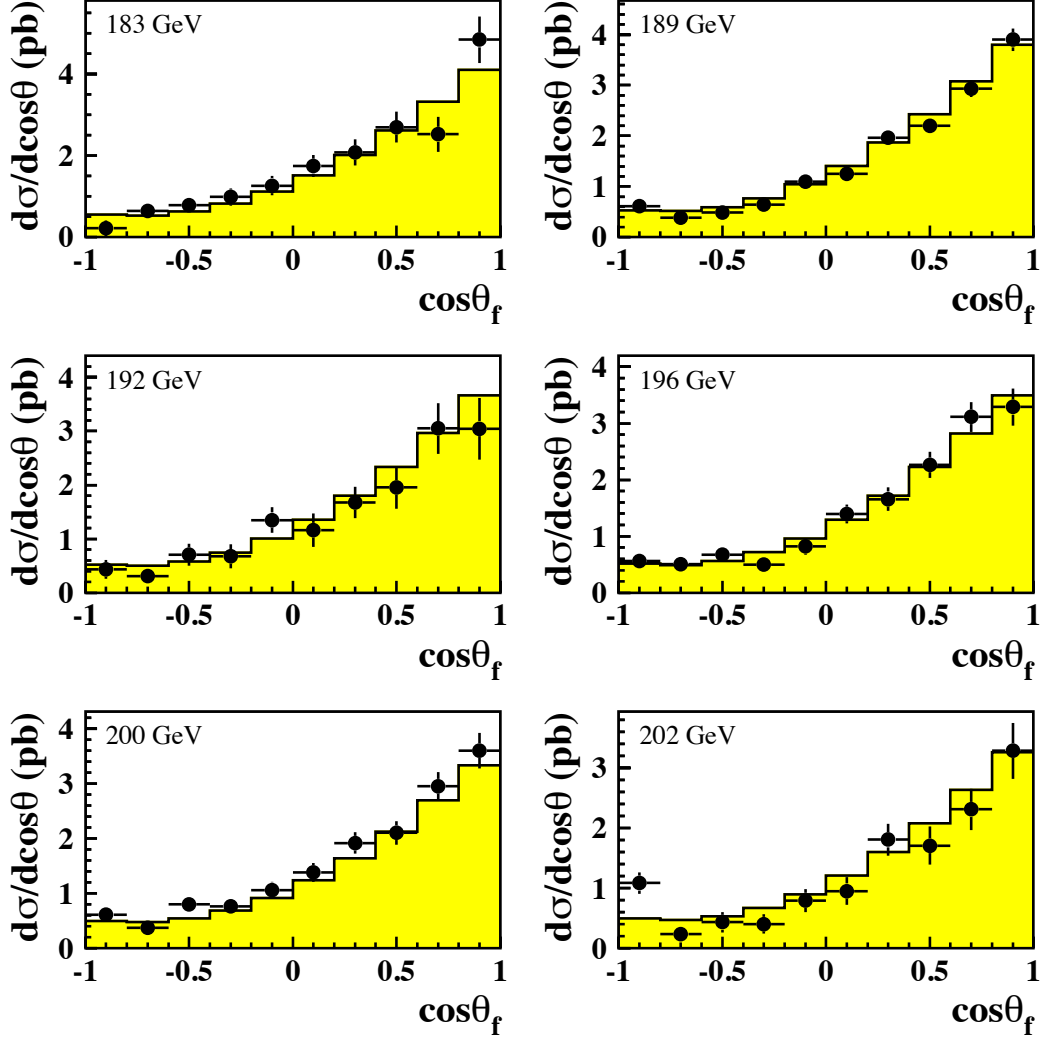


Figure 4: LEP averaged differential cross-sections for  $e^+e^- \rightarrow \mu^+\mu^-$  at energies of 183-202 GeV. The SM predictions, shown as solid histograms, are computed with ZFITTER [5].

## Preliminary LEP Averaged $d\sigma/d\cos\theta$ ( $\tau\tau$ )

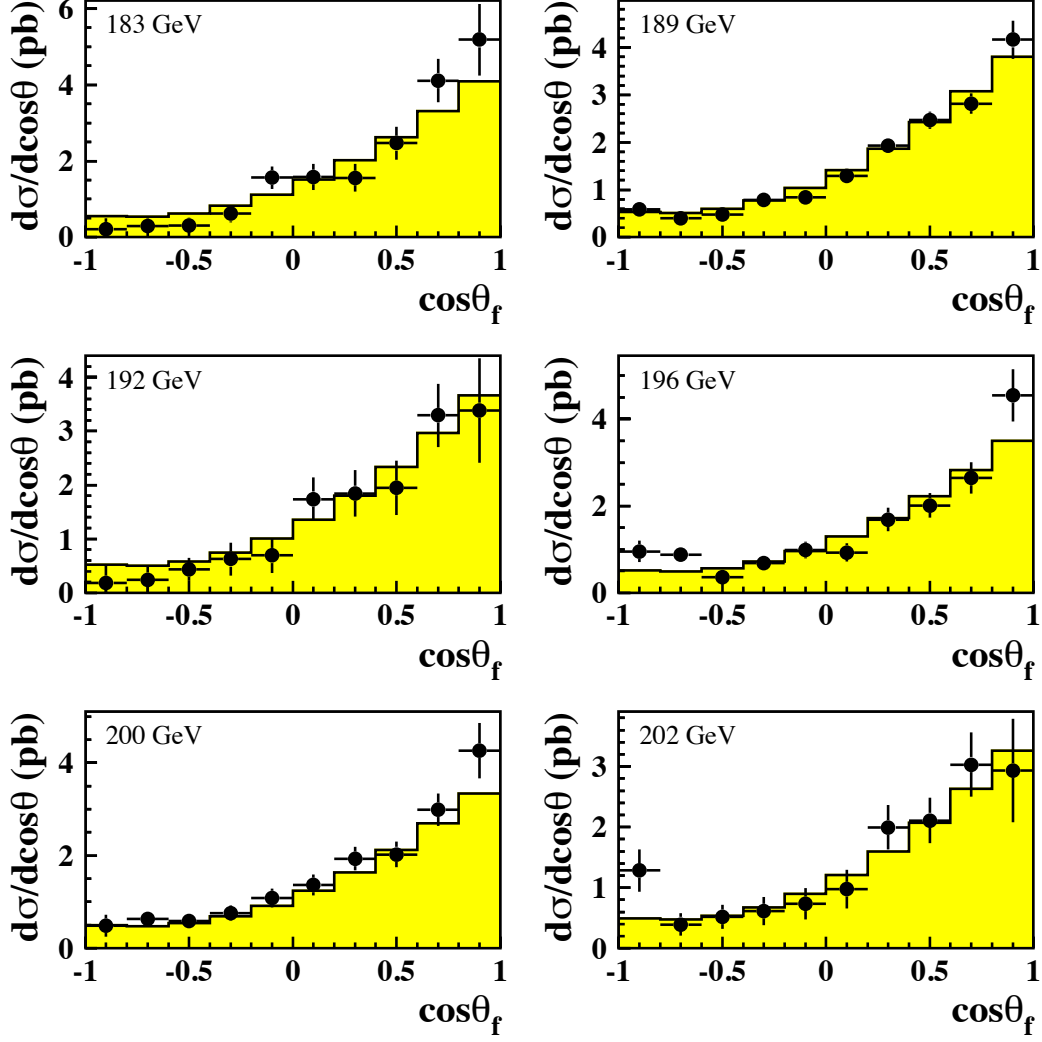


Figure 5: LEP averaged differential cross-sections for  $e^+e^- \rightarrow \tau^+\tau^-$  at energies of 183-202 GeV. The SM predictions, shown as solid histograms, are computed with ZFITTER [5].

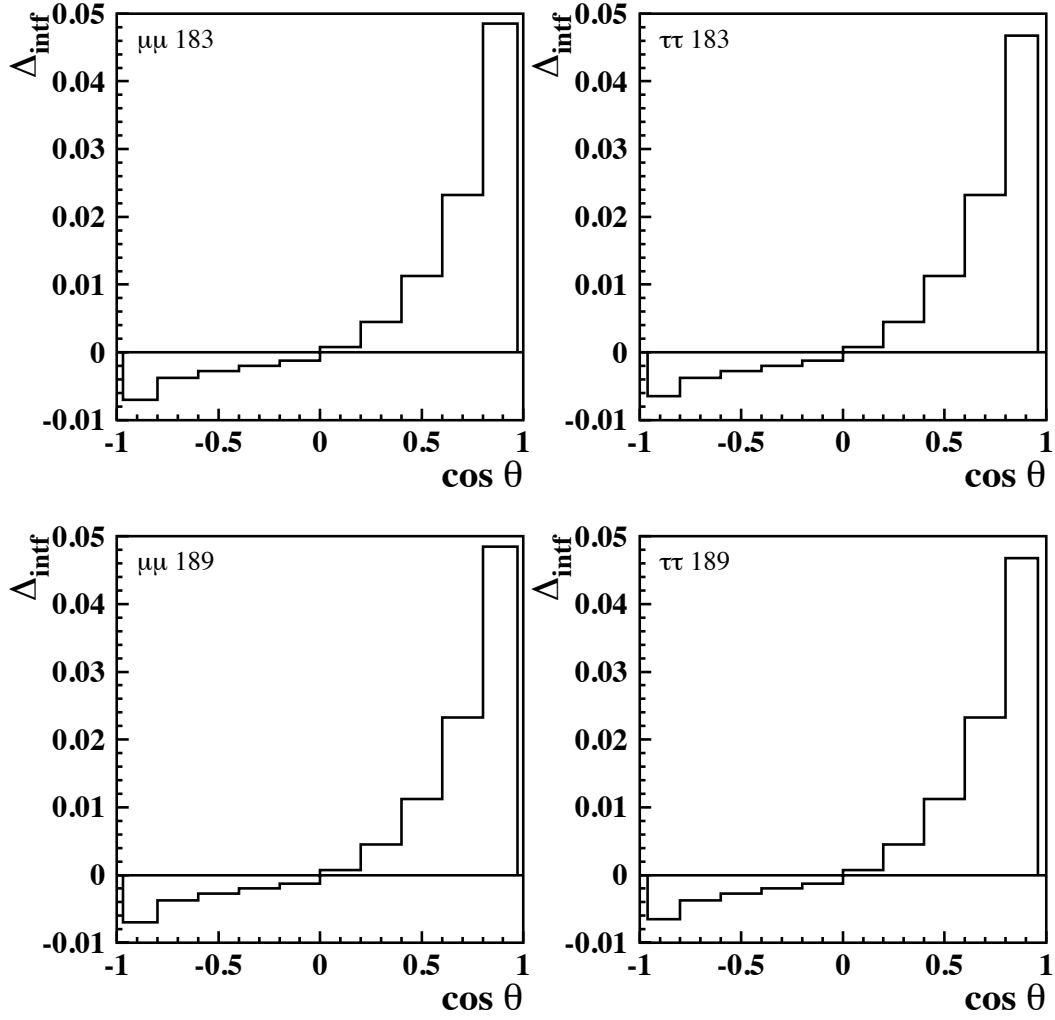


Figure 6: *Difference between predicted differential cross-sections with and without ISR\*FSR interference.*

$\sqrt{s}$ (GeV)	$R_b$				$R_c$				$A_{FB}^b$				$A_{FB}^c$			
	A	D	L	O	A	D	L	O	A	D	L	O	A	D	L	O
133	F	F	F	F	-	-	-	-	-	F	-	F	-	F	-	F
167	F	F	F	F	-	-	-	-	-	F	-	F	-	F	-	F
183	F	P	F	F	F	-	-	-	F	-	-	F	P	-	-	F
189	P	P	F	F	P	-	-	-	P	P	F	F	-	-	-	F
192 to 202	-	P	P	-	-	-	-	-	-	P	-	-	-	-	-	-
206	-	P	-	-	-	-	-	-	-	P	-	-	-	-	-	-

Table 6: Data provided by the ALEPH, DELPHI, L3, OPAL collaborations for combination at different centre-of-mass energies. Data indicated with F are final, published data. Data marked with P are preliminary. Data marked with a - were not supplied for combination.

$\sqrt{s}$ (GeV)	$R_b$	$R_c$	$A_{FB}^b$	$A_{FB}^c$
133	$0.1809 \pm 0.0133$ (0.1853)	- -	$0.357 \pm 0.251$ (0.487)	$0.580 \pm 0.314$ (0.681)
167	$0.1479 \pm 0.0127$ (0.1708)	- -	$0.618 \pm 0.254$ (0.561)	$0.921 \pm 0.344$ (0.671)
183	$0.1616 \pm 0.0101$ (0.1671)	$0.270 \pm 0.043$ (0.250)	$0.527 \pm 0.155$ (0.578)	$0.662 \pm 0.209$ (0.656)
189	$0.1559 \pm 0.0066$ (0.1660)	$0.241 \pm 0.024$ (0.252)	$0.500 \pm 0.096$ (0.583)	$0.462 \pm 0.197$ (0.649)
192	$0.1688 \pm 0.0187$ (0.1655)	- -	$0.371 \pm 0.302$ (0.585)	- -
196	$0.1577 \pm 0.0109$ (0.1648)	- -	$0.721 \pm 0.194$ (0.587)	- -
200	$0.1621 \pm 0.0111$ (0.1642)	- -	$0.741 \pm 0.206$ (0.590)	- -
202	$0.1873 \pm 0.0177$ (0.1638)	- -	$0.591 \pm 0.284$ (0.591)	- -
206	$0.1696 \pm 0.0182$ (0.1633)	- -	$0.881 \pm 0.221$ (0.593)	- -

Table 7: Results of the global fit, compared to the Standard Model predictions, computed with ZFITTER [12], for the signal definition in parentheses. Quoted errors represent the statistical and systematic errors added in quadrature. Because of the large correlation with  $R_c$  at 183 GeV and 189 GeV, the errors on the corresponding measurements of  $R_b$  receive an additional contribution which is absent at the other energy points.

Error list	$R_b$ (189 GeV)	$R_c$ (189 GeV)	$A_{FB}^b$ (189 GeV)	$A_{FB}^c$ (189 GeV)
statistics	0.00606	0.0179	0.0893	0.1771
internal syst	0.00241	0.0128	0.0326	0.0692
common syst	0.00089	0.0092	0.0094	0.0521
total syst	0.00257	0.0158	0.0339	0.0866
total error	0.00659	0.0239	0.0955	0.1971

Table 8: Error breakdown at 189 GeV

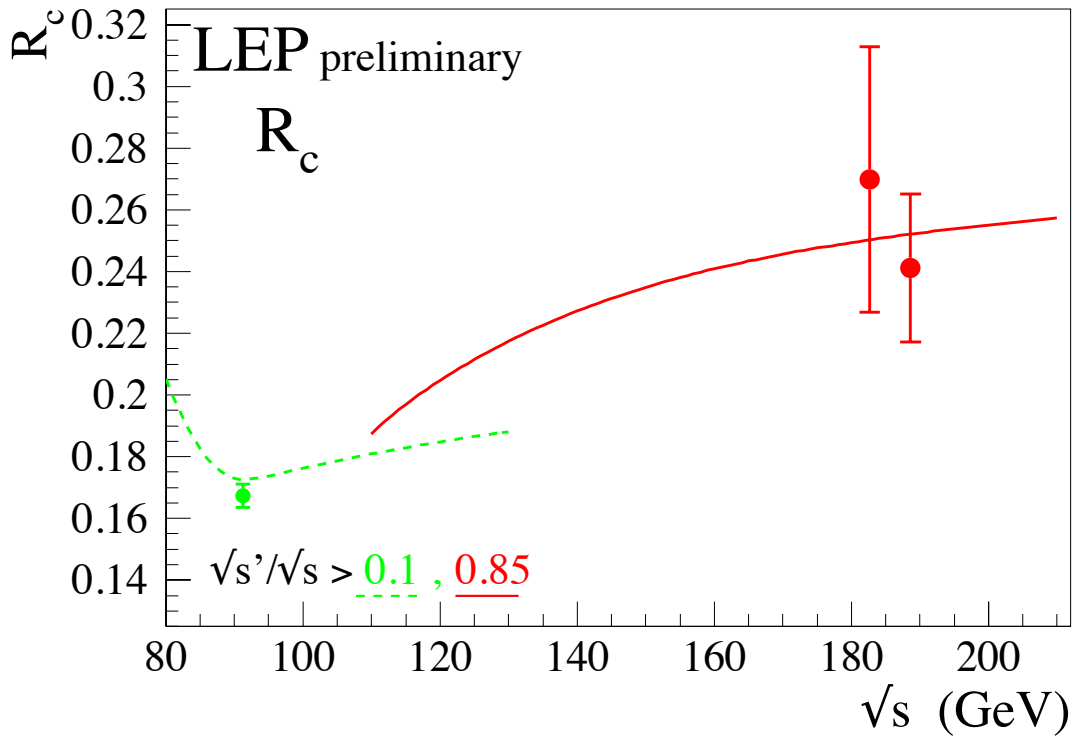
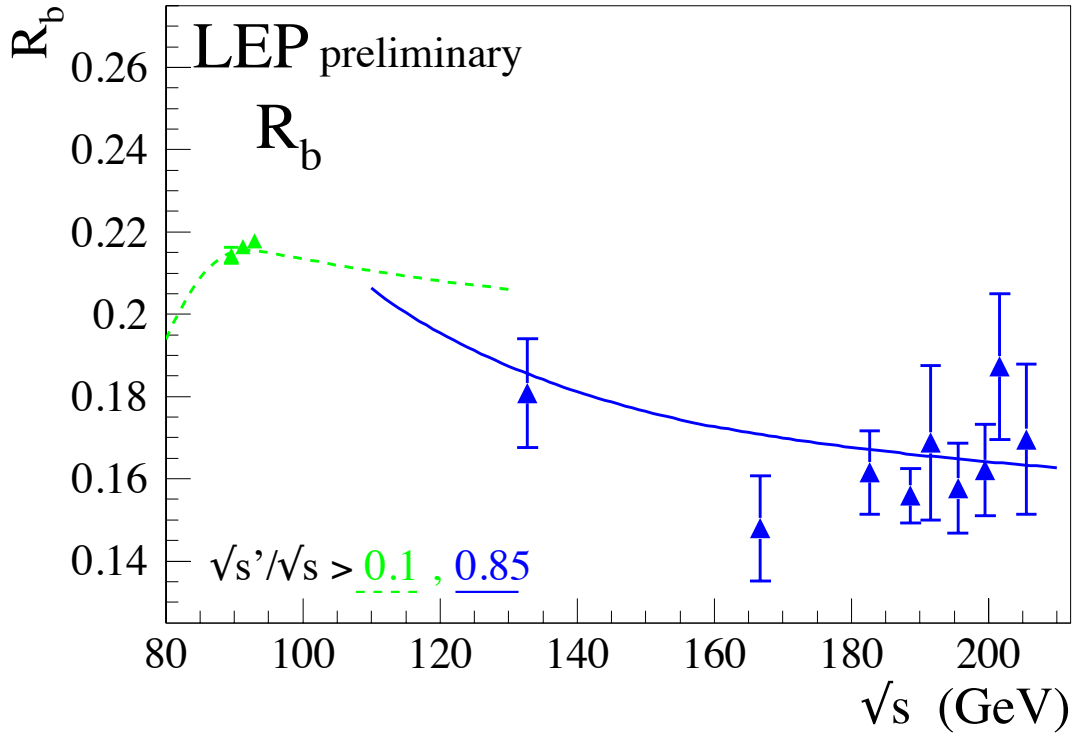


Figure 7: Preliminary combined LEP measurements of  $R_b$  and  $R_c$ . Solid lines represent the Standard Model prediction for the signal definition and dotted lines the inclusive prediction. Both are computed with ZFITTER[12]. The LEP I measurements have been taken from [14].

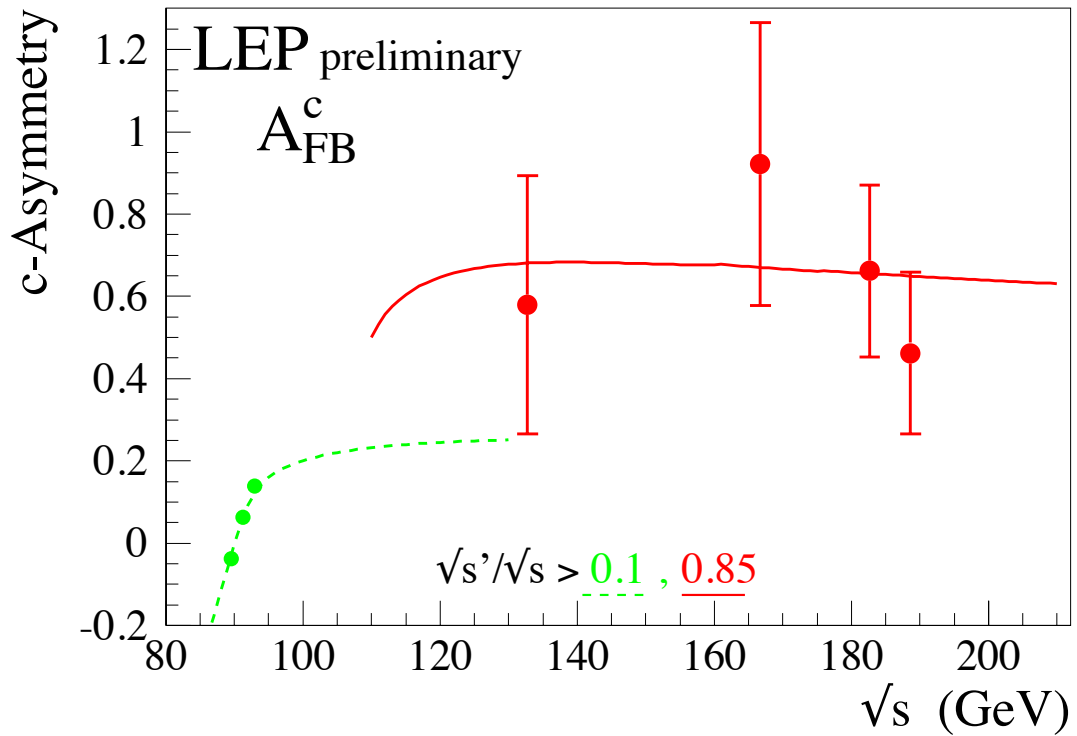
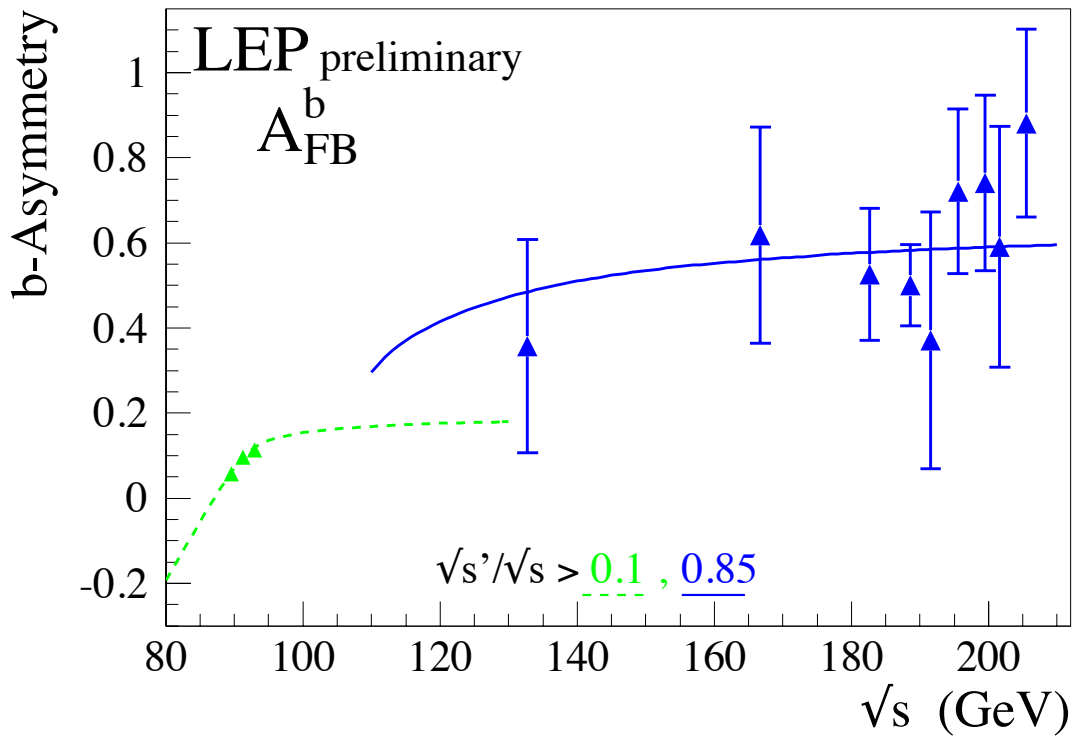


Figure 8: Preliminary combined LEP measurements of the forward-backward asymmetries  $A_{\text{FB}}^b$  and  $A_{\text{FB}}^c$ . Solid lines represent the Standard Model prediction for the signal definition and dotted lines the inclusive prediction. Both are computed with ZFITTER[12]. The LEP I measurements have been taken from [14].

Model	$\chi$	$\psi$	$\eta$	L-R	SSM
$M_{Z'}^{limit}$ (GeV/ $c^2$ )	630	510	400	950	2260

Table 9: 95% confidence level lower limits on the  $Z'$  mass and  $\chi$ ,  $\psi$ ,  $\eta$ , L-R and SSM models.

## 5 Interpretation

The combined cross-sections and asymmetries and results on heavy flavour production have been interpreted in a variety of models. The cross-section and asymmetry results have been used to place limits on the mass of a possible additional heavy neutral boson,  $Z'$ , in several models. Limits on contact interactions between leptons and on contact interaction between electrons and  $b$  and  $c$  quarks have been obtained. Heavy flavour results are also used within the S-Matrix formalism to give information on the  $\gamma - Z$  interference for heavy quarks.

### 5.1 Models with $Z'$ Bosons

The combined hadronic and leptonic cross-sections and the leptonic forward-backward asymmetries were used to fit the data to models including an additional, heavy, neutral boson,  $Z'$  within a variety of models [15].

Fits were made to the mass of a  $Z'$ ,  $M_{Z'}$ , for 4 different models referred to as  $\chi$ ,  $\psi$ ,  $\eta$  and L-R and for the Sequential Standard Model [16], which proposes the existence of a  $Z'$  with exactly the same coupling to fermions as the standard  $Z$ . LEP II data alone does not significantly constrain the the mixing angle between the  $Z$  and  $Z'$  fields,  $\Theta_{ZZ'}$ . However results from a single experiment where LEP I data is used in the fit show that the mixing is consistent with zero, see for example [17]. So for these fits  $\Theta_{ZZ'}$  was fixed to zero.

No evidence was found for the existence of a  $Z'$  boson in any of the models.

95% confidence level lower limits on  $M_{Z'}$  were obtained, by integrating the likelihood function<sup>†</sup>. The lower limits on the  $Z'$  mass are shown in Table 9.

### 5.2 Contact Interactions between Leptons

Following reference [18], contact interactions are parameterised by an effective Lagrangian,  $\mathcal{L}_{\text{eff}}$ , which is added to the Standard Model Lagrangian and has the form:

$$\mathcal{L}_{\text{eff}} = \frac{g^2}{(1 + \delta)\Lambda^2} \sum_{i,j=L,R} \eta_{ij} \bar{e}_i \gamma_\mu e_i \bar{f}_j \gamma^\mu f_j,$$

where  $g^2/4\pi$  is taken to be 1 by convention,  $\delta = 1(0)$  for  $f = e(f \neq e)$ ,  $\eta_{ij} = \pm 1$  or 0,  $\Lambda$  is the scale of the contact interactions,  $e_i$  and  $f_j$  are left or right-handed spinors. By assuming different helicity coupling between the initial state and final state currents a set of different models can be defined from this Lagrangian [19], with either constructive (+) or destructive (−) interference between the Standard Model process and the contact interactions. The models and corresponding choices of  $\eta_{ij}$  are given in Table 10. The models LL, RR, VV, AA, LR, RL, V0, A0 are considered here since these models lead to large deviations in the  $e^+e^- \rightarrow \mu^+\mu^-$  and

<sup>†</sup>To be able to obtain confidence limits from the likelihood function it is necessary to convert the likelihood to a probability density function; this is done by multiplying by a prior probability function. Simply integrating the likelihood is equivalent to multiplying by a uniform prior probability function.

$e^+e^- \rightarrow \tau^+\tau^-$  channels. The total hadronic cross-section on its own is not particularly sensitive to contact interactions involving quarks. For the purpose of fitting contact interaction models to the data, a new parameter  $\epsilon = 1/\Lambda^2$  is defined;  $\epsilon = 0$  in the limit that there are no contact interactions. This parameter is allowed to take both positive and negative values in the fits.

The averaged measurements of the cross-sections and forward-backward asymmetries for  $e^+e^- \rightarrow \mu^+\mu^-$  and  $e^+e^- \rightarrow \tau^+\tau^-$  from all energies from 130 to 207 GeV have been used. Theoretical uncertainties on the SM predictions of  $\pm 0.5\%$  [8] on the cross-sections and  $\pm 0.005$  on the forward-backward asymmetries, fully correlated between all energies, have been assumed.

The values of  $\epsilon$  extracted for each model were all compatible with the Standard Model expectation  $\epsilon = 0$ , at the two standard deviation level. These errors on  $\epsilon$  are typically a factor of two smaller than those obtained from a single LEP experiment with the same data set. The fitted values of  $\epsilon$  were converted into 95% confidence level lower limits on  $\Lambda$ . The limits are obtained by integrating the likelihood function over the physically allowed values,  $\epsilon \geq 0$  for each  $\Lambda^+$  limit and  $\epsilon \leq 0$  for  $\Lambda^-$  limits. The fitted values of  $\epsilon$  and the extracted limits are shown in Table 11. Figure 9 shows the limits obtained on the scale  $\Lambda$  for the different models assuming universality between contact interactions for  $e^+e^- \rightarrow \mu^+\mu^-$  and  $e^+e^- \rightarrow \tau^+\tau^-$ .

### 5.3 Contact Interactions from Heavy Flavour Averages

Limits on contact interactions between electrons and  $b$  and  $c$  quarks have been obtained. These results are of particular interest since they are inaccessible to  $p\bar{p}$  or  $ep$  colliders. The formalism for describing contact interactions including heavy flavours is identical to that described above for leptons.

All heavy flavour LEP II combined results from 133 to 205 GeV listed in Table 7 are used as inputs. For the purpose of fitting contact interaction models to the data,  $R_b$  and  $R_c$  are converted to cross-sections  $\sigma_{b\bar{b}}$  and  $\sigma_{c\bar{c}}$  using the averaged  $q\bar{q}$  cross-section of section 2 corresponding to signal definition 2. In the calculation of errors, the correlations between  $R_b$ ,  $R_c$  and  $\sigma_{q\bar{q}}$  are assumed to be negligible.

The fitted values of  $\epsilon = \frac{1}{\Lambda^2}$  and their 68% confidence level uncertainties together with the 95% confidence level lower limit on  $\Lambda$  are shown in Table 12. Figure 10 shows the limits obtained on the scale,  $\Lambda$ , of models with different helicity combinations involved in the interactions.

### 5.4 S-Matrix Parameters for Heavy Flavour Production

The S-Matrix formalism [20] parameterises the cross-sections and forward-backward asymmetries for two-fermion production in terms of the exchange of a massless ( $\gamma$ ) and a massive vector boson ( $Z$ ):

$$\sigma_{tot}^{0,f}(s) = \frac{4}{3}\pi\alpha^2 + \left[ \frac{g_f^{tot}}{s} + \frac{j_f^{tot}(s - \overline{m}_Z^2) + r_f^{tot}s}{(s - \overline{m}_Z^2)^2 + \overline{m}_Z^2\overline{\Gamma}_Z^2} \right]$$

$$\sigma_{fb}^{0,f}(s) = \frac{4}{3}\pi\alpha^2 + \left[ \frac{g_f^{fb}}{s} + \frac{j_f^{fb}(s - \overline{m}_Z^2) + r_f^{fb}s}{(s - \overline{m}_Z^2)^2 + \overline{m}_Z^2\overline{\Gamma}_Z^2} \right]$$

$$A_{fb}^{0,f}(s) = \frac{3\sigma_{fb}^{0,f}(s)}{4\sigma_{tot}^{0,f}(s)}$$

Model	$\eta_{LL}$	$\eta_{RR}$	$\eta_{LR}$	$\eta_{RL}$
LL $^\pm$	$\pm 1$	0	0	0
RR $^\pm$	0	$\pm 1$	0	0
VV $^\pm$	$\pm 1$	$\pm 1$	$\pm 1$	$\pm 1$
AA $^\pm$	$\pm 1$	$\pm 1$	$\mp 1$	$\mp 1$
LR $^\pm$	0	0	$\pm 1$	0
RL $^\pm$	0	0	0	$\pm 1$
V0 $^\pm$	$\pm 1$	$\pm 1$	0	0
A0 $^\pm$	0	0	$\pm 1$	$\pm 1$

Table 10: Choices of  $\eta_{ij}$  for different contact interaction models

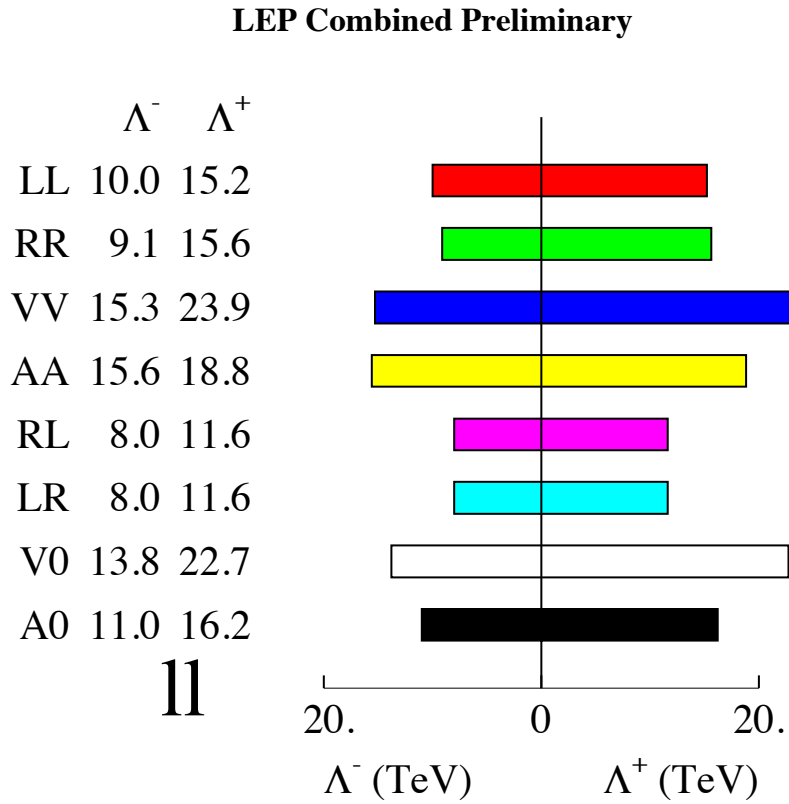


Figure 9: The limits on  $\Lambda$  for  $e^+e^- \rightarrow \ell^+\ell^-$  assuming universality in the contact interactions between  $e^+e^- \rightarrow \mu^+\mu^-$  and  $e^+e^- \rightarrow \tau^+\tau^-$ .

$e^+e^- \rightarrow \mu^+\mu^-$			
Model	$\epsilon$ (TeV $^{-2}$ )	$\Lambda^-$ (TeV)	$\Lambda^+$ (TeV)
LL	$-0.0066^{+0.0039}_{-0.0042}$	8.2	14.3
RR	$-0.0069^{+0.0045}_{-0.0054}$	8.0	13.4
VV	$-0.0023^{+0.0017}_{-0.0018}$	13.7	21.6
AA	$-0.0033^{+0.0032}_{-0.0012}$	13.1	19.2
RL	$-0.0052^{+0.0067}_{-0.0074}$	7.2	10.1
LR	$-0.0052^{+0.0067}_{-0.0074}$	7.2	10.1
V0	$-0.0036^{+0.0024}_{-0.0022}$	11.9	20.6
A0	$-0.0027^{+0.0035}_{-0.0033}$	10.8	14.4

$e^+e^- \rightarrow \tau^+\tau^-$			
Model	$\epsilon$ (TeV $^{-2}$ )	$\Lambda^-$ (TeV)	$\Lambda^+$ (TeV)
LL	$-0.0005^{+0.0057}_{-0.0055}$	9.5	9.8
RR	$-0.0005^{+0.0060}_{-0.0063}$	8.7	9.5
VV	$-0.0008^{+0.0023}_{-0.0036}$	14.4	16.1
AA	$-0.0008^{+0.0033}_{-0.0016}$	13.4	12.2
RL	$-0.0052^{+0.0093}_{-0.0102}$	6.5	8.8
LR	$-0.0052^{+0.0093}_{-0.0102}$	6.5	8.8
V0	$-0.0003^{+0.0029}_{-0.0029}$	12.9	13.7
A0	$-0.0026^{+0.0049}_{-0.0050}$	9.5	12.4

$e^+e^- \rightarrow l^+l^-$			
Model	$\epsilon$ (TeV $^{-2}$ )	$\Lambda^-$ (TeV)	$\Lambda^+$ (TeV)
LL	$-0.0046^{+0.0038}_{-0.0036}$	10.0	15.2
RR	$-0.0046^{+0.0038}_{-0.0044}$	9.1	15.6
VV	$-0.0019^{+0.0024}_{-0.0012}$	15.3	23.9
AA	$-0.0013^{+0.0018}_{-0.0015}$	15.6	18.8
RL	$-0.0052^{+0.0054}_{-0.0060}$	8.0	11.6
LR	$-0.0052^{+0.0054}_{-0.0060}$	8.0	11.6
V0	$-0.0023^{+0.0018}_{-0.0020}$	13.8	22.7
A0	$-0.0027^{+0.0028}_{-0.0028}$	11.0	16.2

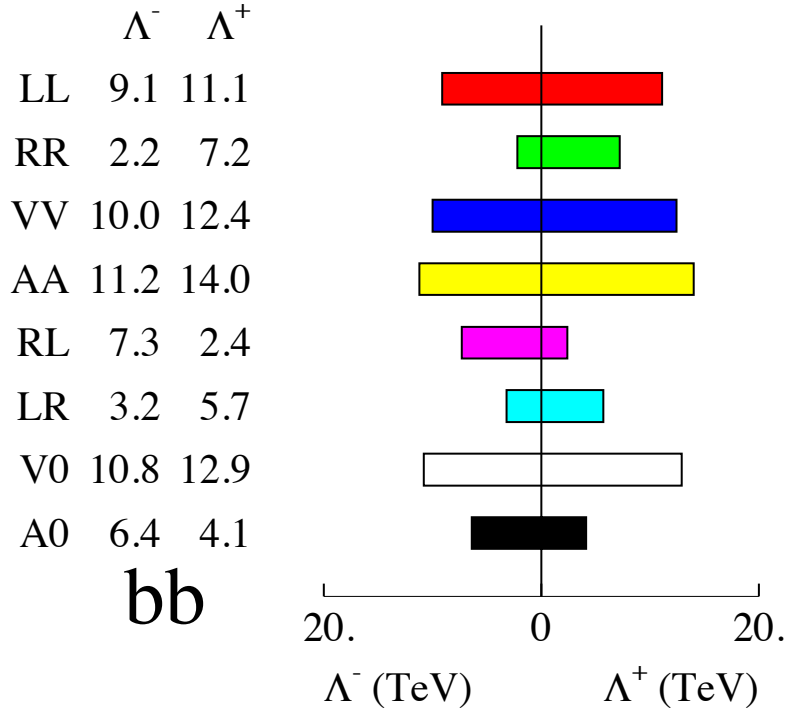
Table 11: *Fitted values of  $\epsilon$  and 95% confidence limits on the scale,  $\Lambda$ , for constructive (+) and destructive interference (-) with the Standard Model, for the contact interaction models discussed in the text. Results are given for  $e^+e^- \rightarrow \mu^+\mu^-$ ,  $e^+e^- \rightarrow \tau^+\tau^-$  and  $e^+e^- \rightarrow \ell^+\ell^-$ , assuming universality in the contact interactions between  $e^+e^- \rightarrow \mu^+\mu^-$  and  $e^+e^- \rightarrow \tau^+\tau^-$ .*

$e^+e^- \rightarrow b\bar{b}$			
Model	$\epsilon$ (TeV <sup>-2</sup> )	$\Lambda^-$ (TeV)	$\Lambda^+$ (TeV)
LL	$-0.0025^{+0.0049}_{-0.0052}$	9.1	11.1
RR	$-0.1890^{+0.1290}_{-0.0151}$	2.2	7.2
VV	$-0.0020^{+0.0041}_{-0.0043}$	10.0	12.4
AA	$-0.0018^{+0.0032}_{-0.0034}$	11.2	14.0
RL	$0.0190^{+0.1299}_{-0.0201}$	7.3	2.4
LR	$-0.0428^{+0.0408}_{-0.0367}$	3.2	5.7
V0	$-0.0018^{+0.0035}_{-0.0037}$	10.8	12.9
A0	$0.0266^{+0.0234}_{-0.0255}$	6.4	4.1

$e^+e^- \rightarrow c\bar{c}$			
Model	$\epsilon$ (TeV <sup>-2</sup> )	$\Lambda^-$ (TeV)	$\Lambda^+$ (TeV)
LL	$0.0127^{+0.5957}_{-0.0264}$	5.2	1.6
RR	$0.0466^{+0.3781}_{-0.0576}$	4.5	1.5
VV	$-0.0008^{+0.0109}_{-0.0103}$	7.3	6.6
AA	$0.0046^{+0.0168}_{-0.0151}$	6.4	5.1
RL	$0.0127^{+0.0845}_{-0.0845}$	2.8	2.6
LR	$0.0874^{+0.1049}_{-0.1127}$	3.5	2.1
V0	$0.0036^{+0.0181}_{-0.0135}$	6.7	1.4
A0	$0.0499^{+0.0691}_{-0.0691}$	3.9	2.6

Table 12: *Fitted values of  $\epsilon$  and 95% confidence limits on the scale,  $\Lambda$ , for constructive (+) and destructive interference (-) with the Standard Model, for the contact interaction models discussed in the text. From combined  $b\bar{b}$  and  $c\bar{c}$  results with centre of mass energies from 133 to 205 GeV.*

LEP Combined Preliminary



LEP Combined Preliminary

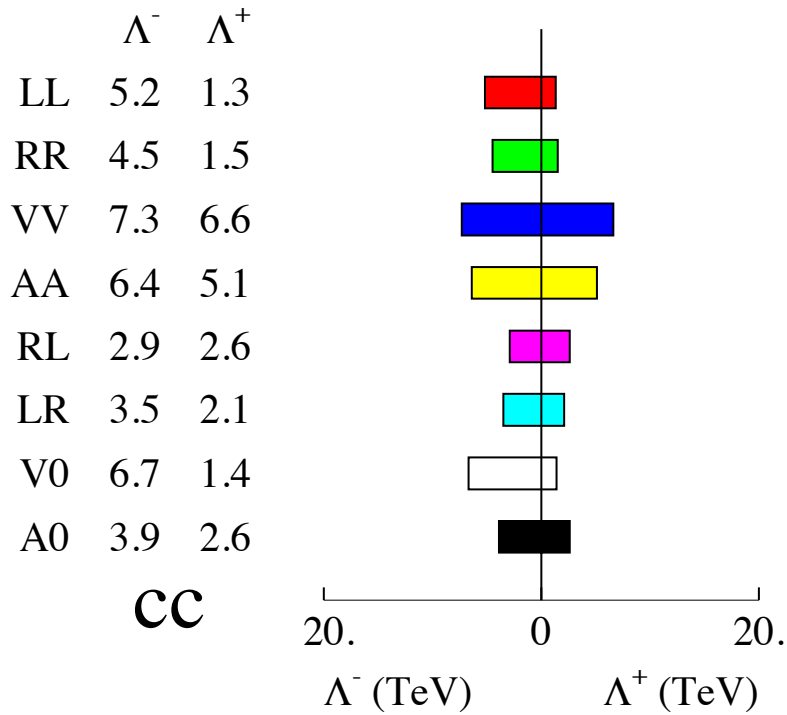


Figure 10: 95% CL limits on the scale of Contact Interactions in  $e^+e^- \rightarrow b\bar{b}$  and  $e^+e^- \rightarrow c\bar{c}$  using Heavy Flavour LEP combined results from 133 to 205 GeV.

The mass,  $\overline{m}_z$ , and width,  $\overline{\Gamma}_Z$ , used in the S-Matrix fits are slightly different from the usual mass  $M_Z$ , and width  $\Gamma_Z$  which are defined using an  $s$ -dependent width term in the Breit-Wigner resonance of the Z:

$$\begin{aligned}\overline{m}_z &\sim M_Z - 34.1\text{MeV} \\ \overline{\Gamma}_z &\sim \Gamma_Z - 0.9\text{MeV}\end{aligned}$$

The parameters  $g$ ,  $r$  and  $j$  parameterise the cross-sections and forward-backward asymmetries arising from the exchange of the  $\gamma$  ( $g$ ) and the Z ( $r$ ) and the interference of the two ( $j$ ). Values for these parameters can be obtained for each fermion species and also for a combination of all  $q\bar{q}$  final states,  $f = had$ . Values of the  $g$ ,  $r$  and  $j$  parameters and  $\overline{\gamma}_z$  can be computed in the Standard Model for comparison with the results of the fits.

S-Matrix fits have already been performed using the hadronic and leptonic cross-section and leptonic forward-backward asymmetry data from LEP I and LEP II for energies up to 172 GeV [21], providing constraints on  $r_{had}^{tot}$  and  $j_{had}^{tot}$ , the parameters describing charged lepton production and  $\overline{m}_z$  and  $\overline{\Gamma}_Z$ . The results of these existing fits and the full error matrix are used to constrain these parameters in the fit performed here.

LEP I heavy flavour averages [22],  $R_b$ ,  $R_c$ ,  $A_{FB}^b$  and  $A_{FB}^c$  are used to constrain the S-Matrix parameters  $r_{b,c}^{tot}$  and  $r_{b,c}^{fb}$  that describe the heavy quark couplings to the Z. By including the combined LEP II heavy flavour measurements from 133 to 205 GeV listed in Table 7 values of the parameters  $j_{b,c}^{tot}$  and  $j_{b,c}^{fb}$  that describe  $\gamma - Z$  interference in heavy quark production are obtained. Contours for these parameters are given at the end of this section.

The LEP II average values of  $R_b$  and  $R_c$  from Section 4 for centre-of-mass energies from 130 up to 166 GeV are used directly in the fit. These are largely uncorrelated with the measured total cross-sections, therefore, the correlations between the existing S-Matrix fits parameters and these measurements have been neglected. The measurements are fitted using the ratio of the predicted  $b$  and  $c$  cross-sections and the total hadronic cross-section.

For energies of 183 GeV and above, the the flavour tagged measurements are more precise than those from 133–166 GeV. The uncertainties on  $j_{had}^{tot}$  from the existing fits introduces a sizeable uncertainty of the prediction of  $R_b$  and  $R_c$ . For these energies the measurements of  $R_b$  and  $R_c$  are first converted into cross-sections for  $b\bar{b}$  and  $c\bar{c}$  production by multiplying by the the total hadronic cross-sections from section 2. The full error matrix of the quantities and the correlations with the lower energy  $R_b$  and  $R_c$  values are computed. Correlations between the existing S-Matrix fit results and the total hadronic cross-sections from 183 GeV and above are neglected. For this reason the highest energy hadronic cross-sections were not used to improve the fits to the inclusive hadronic S-Matrix parameters.

The forward-backward asymmetries for  $b$  and  $c$  quark production are fitted directly to predictions of the asymmetries at all energies.

Predictions of the S-Matrix formalism are made using the SMATASY [23] program. The couplings to the photon are fixed to the expectation from the Standard Model.

In summary, the following parameters are obtained from the fit:

- The mass and total width of the Z boson, the S-Matrix parameters  $r_{had}^{tot}$  and  $j_{had}^{tot}$  for the total hadronic cross-section, and the parameters  $r_1^{tot}$ ,  $j_1^{tot}$ ,  $r_1^{fb}$ , and  $j_1^{fb}$  for leptons<sup>‡</sup>.
- The S-Matrix parameters  $r_{b,c}^{tot}$  and  $r_{b,c}^{fb}$  that describe the total  $b\bar{b}$  and  $c\bar{c}$  cross-sections and asymmetries due to Z boson exchange.
- The four parameters  $j_{b,c}^{tot}$  and  $j_{b,c}^{fb}$  that describe the the effect of  $\gamma - Z$  interference on the energy dependence of the bottom and charm cross-sections and asymmetries.

---

<sup>‡</sup>Lepton universality is assumed.

The following data are used:

- The results of the existing S-Matrix fits [21], derived from LEP I data and including total hadronic cross-sections up to 172 GeV.
- LEP I heavy flavour averages [22].
- LEP II heavy flavour averages  $R_b$  and  $R_c$  for energies up to and including 172 GeV from Table 7.
- Values of the flavour tagged b and c cross-sections  $\sigma_b$  and  $\sigma_c$  derived from measurements of  $R_b$  and  $R_c$  and the total hadronic cross-section for energies of 183 GeV and above, from section 2 and Table 7.
- LEP II heavy flavour averages  $A_{\text{FB}}^b$  and  $A_{\text{FB}}^c$  for all LEP II energies from Table 7.

The results for the S-Matrix parameters  $j_{b,c}^{\text{tot}}$  and  $j_{b,c}^{\text{fb}}$  are shown in Figure 11 for both bottom and charm quark production. Good agreement is observed with the Standard Model prediction [23] for  $\gamma - Z$  interference in heavy quark production.

## 6 Summary

A preliminary combination of the LEP II  $e^+e^- \rightarrow f\bar{f}$  cross-sections (for hadron, muon and tau final states) and forward-backward asymmetries (for muon and tau final states) from LEP running at energies from 130 to 207 GeV has been made. The results from the four LEP experiments are in good agreement with each other. The results for energies between 192 and 202 GeV are given in Table 2, results for 130–189 GeV are available in [1]. The averages for all energies are shown graphically in Figures 1 and 2. Overall the data agree with the Standard Model predictions of ZFITTER, although the combined hadronic cross-sections are on average 2.5 standard deviations above the predictions.

For the first time differential cross-sections,  $\frac{d\sigma}{d\cos\theta}$ , for  $e^+e^- \rightarrow \mu^+\mu^-$  and  $e^+e^- \rightarrow \tau^+\tau^-$  were combined. Results are shown in Figures 4 and 5.

An average of results on heavy flavour production at LEP II has also been made for measurements of  $R_b$ ,  $R_c$ ,  $A_{\text{FB}}^b$  and  $A_{\text{FB}}^c$ , using results from LEP centre-of-mass energies from 130 to 209 GeV. Results are given in Table 7 and shown graphically in Figures 7 and 8. The results are in good agreement with the predictions of the SM. Further details are given in [11].

The averaged cross-section and forward-backward asymmetry results together with the combined results on heavy flavour production were interpreted in a variety of models. The LEP II averaged cross-sections were used to obtain lower limits on the mass of a possible  $Z'$  boson in different models. Limits range from 400 to 2260 GeV depending on the model. Limits on the scale of contact interactions between leptons and also between electrons and  $b\bar{b}$  and  $c\bar{c}$  final states have been determined. A full set of limits are given in Tables 11 and 12. The heavy flavour results were used to derive values of the S-Matrix parameters  $j_{b,c}^{\text{tot}}$  and  $j_{b,c}^{\text{fb}}$  that describe  $\gamma - Z$  interference, results are given in Figure 11.

## Acknowledgements

The analysis and interpretation of the high energy  $f\bar{f}$  data requires the theoretical input from Monte Carlo programs to compute efficiencies, from programs to compute the luminosity and programs which make Standard Model predictions. We would like to acknowledge the work of all the authors of these programs. In particular we are grateful to D. Bardin, S. Jadach, G. Passarino and B. Ward for their direct contributions to our work.

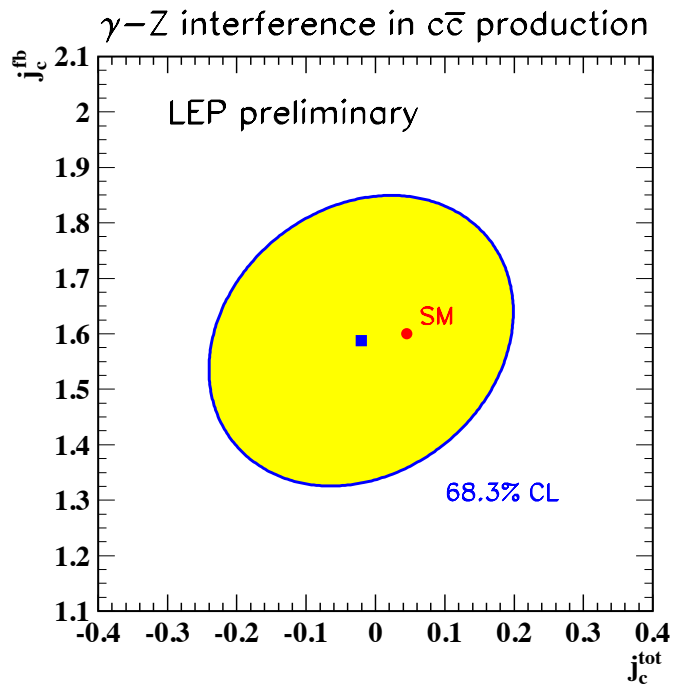
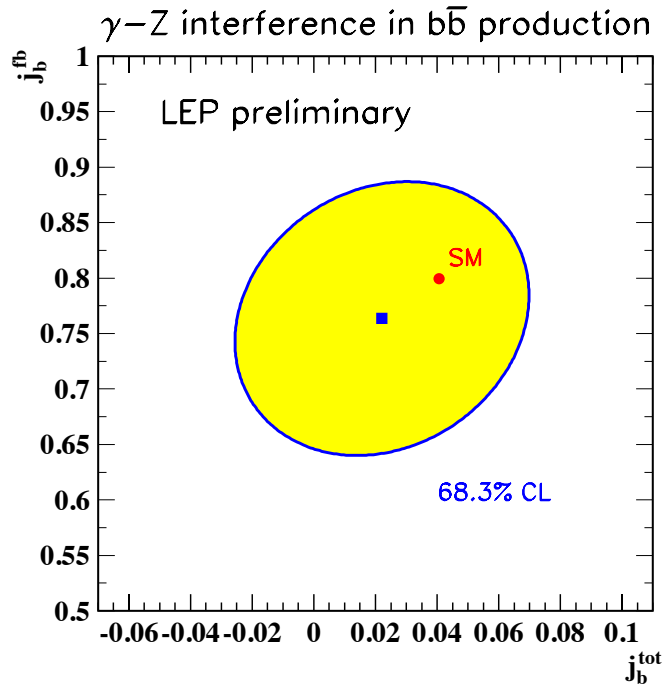


Figure 11: Preliminary combined LEP results on the  $S$ -Matrix parameters describing  $\gamma - Z$  interference in  $b\bar{b}$  and  $c\bar{c}$  production. The expectations of the SM are also shown.

## A Averaging Differential Cross-sections

To investigate the performance of three different methods to average the LEP differential cross-section results an ensemble of 10,000 LEP runs at 183 and 189 GeV was simulated. For each simulated LEP run:

- The expected number of events for 4 experiments for muons and taus in the most backward bin was computed from:

$$N_{signal} = \mathcal{L}\epsilon \left. \frac{d\sigma}{d\cos\theta} \right|_{SM} \Delta \cos\theta \quad (1)$$

$$N_{predicted} = N_{signal} + N_{background} \quad (2)$$

where  $\left. \frac{d\sigma}{d\cos\theta} \right|_{SM}$  is the SM differential cross-section for the experimental signal definition,  $\Delta \cos\theta$  is the width of the bin, for the experiment,  $\epsilon$  is the experiments efficiency for signal events and  $\mathcal{L}$  is the integrated luminosity.

- For each experiment a random number of observed events was generated according to a Poisson distribution with the mean given by  $N_{predicted}$ .
- From the number of observed events the following were computed:
  - the measured differential cross-sections
  - the measured errors - using the square root of the observed events
- From the predicted number of signal and background events the expected error on the differential cross-section for each experiment was computed from:

$$\Delta = \left. \frac{d\sigma}{d\cos\theta} \right|_{SM} \sqrt{N_{predicted}/N_{signal}^2}$$

- Three averages of the differential cross-section were calculated by performing three fits
  - Likelihood fit to observed numbers of events using Poisson probabilities from the expected number of events calculated using equation 2 and  $n_{signal}$  computed from equation 1 with  $\left. \frac{d\sigma}{d\cos\theta} \right|_{SM}$  replaced with the average differential cross-section
  - $\chi^2$  fit to measured  $\left. \frac{d\sigma}{d\cos\theta} \right|_{SM}$  using expected error
  - $\chi^2$  fit to measured  $\left. \frac{d\sigma}{d\cos\theta} \right|_{SM}$  using measured error

DELPHI and OPAL provided  $\epsilon$  and  $\mathcal{L}$  and  $N_{bkg}$ , the DELPHI numbers were also used for ALEPH and the OPAL numbers were also used for L3. The Standard Model cross-sections corresponding to the experimental selections were provided by each of the four experiments.

As in the final fits, the averaged cross-sections correspond to a standard signal definition. For the likelihood fits the average cross-sections were corrected to the experimental definitions before making predictions for the number of expected events. For the  $\chi^2$  fits the measured cross-sections were corrected back to the common signal definition.

Pull distributions were determined for each of the fits over the ensemble of runs using:

$$\text{Pull} = \frac{\left( \left. \frac{d\sigma}{d\cos\theta} \right|_{fit} - \left. \frac{d\sigma}{d\cos\theta} \right|_{SM} \right)}{\Delta_{fit}}$$

$\mu\mu$  183 bin 1

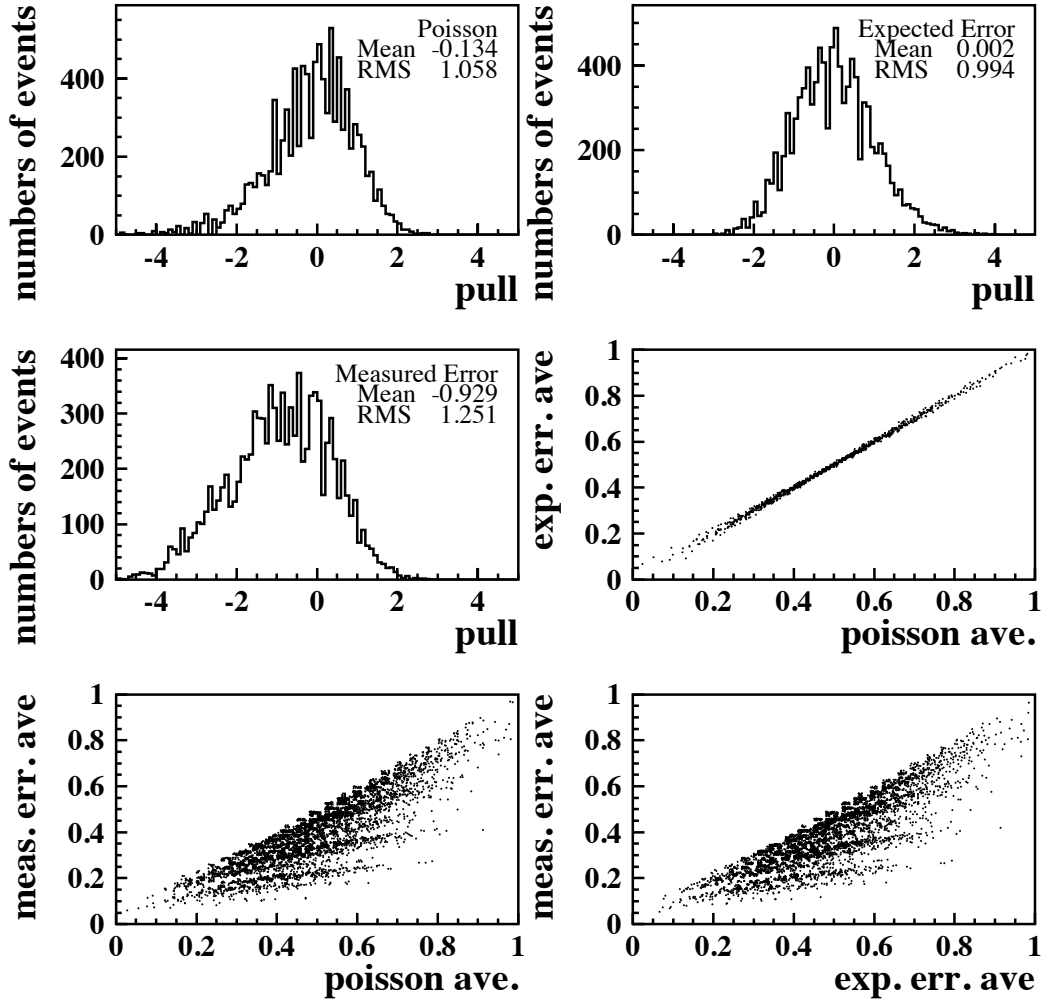


Figure 12: Pull distributions for each fit and the correlations between the results of each fit for muon final states at 183 GeV.

### $\tau\tau$ 183 bin 1

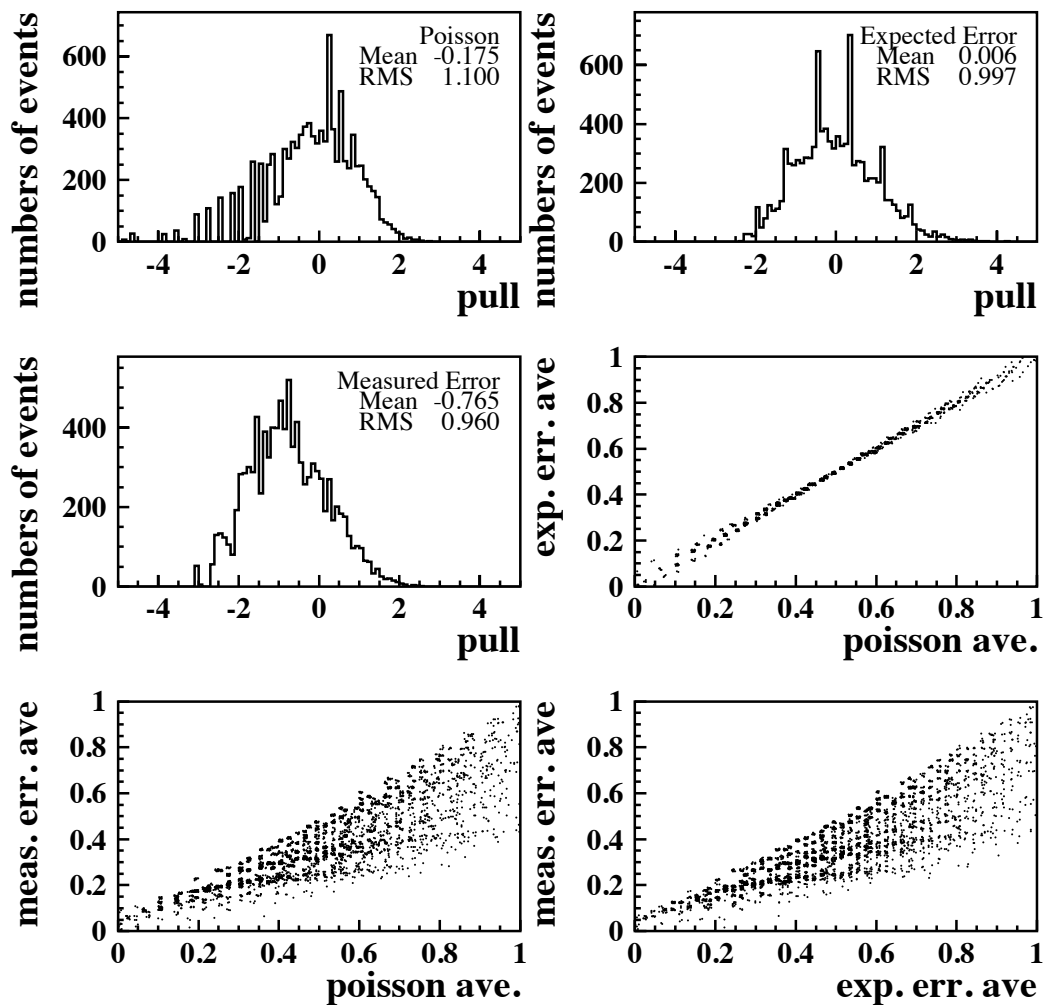


Figure 13: Pull distributions for each fit and the correlations between the results of each fit for tau lepton final states at 183 GeV.

where  $\Delta_{fit}$  is the error on  $\left. \frac{d\sigma}{d\cos\theta} \right|_{fit}$  for a given fit

Figures 12 and 13 show the pull distributions for each fit and the correlations between the results of each fit. The pull distributions for the  $\chi^2$  fit using measured errors show a bias towards low values of the average differential cross-section, with a negative mean. The  $\chi^2$  fits using expected errors have well behaved pull distributions, with a mean close to zero and an rms of approximately one. There is a strong correlation between the results of the  $\chi^2$  fit using expected errors and the likelihood fit with Poisson probabilities of the number of observed events given the numbers expected, whereas the  $\chi^2$  fit using measured errors tend to give lower results than the likelihood fit.

From these studies it was concluded that an average computed from a  $\chi^2$  fit to the differential cross-section in a given bin using the expected error on the differential cross-section was a good approximation to a likelihood fit with Poisson probabilities of the number of observed events given the numbers expected. The  $\chi^2$  fit also has an advantage: it is simple to include uncorrelated systematic errors and systematic errors correlated between measurements into the averaging.

## References

- [1] LEPEWWG  $f\bar{f}$  Subgroup, D. Bourilkov *et al.*, LEP2FF/00-01, ALEPH 2000-026 PHYSIC 2000-005, DELPHI 2000-046 PHYS 855, L3 note 2527, OPAL TN647.
- [2] LEPEWWG  $f\bar{f}$  Subgroup, D. Bourilkov *et al.*, LEP2FF/99-01, ALEPH 99-082 PHYSIC 99-030, DELPHI 99-143 PHYS 829, L3 note 2443, OPAL TN616.
- [3] LEPEWWG  $f\bar{f}$  subgroup: <http://www.cern.ch/LEPEWWG/lep2/> .
- [4] ALEPH Collab., "*Fermion Pair Production in  $e^+e^-$  Collisions from 192 to 202 GeV*", ALEPH 2000-025 CONF 2000-021;  
DELPHI Collab., "*Measurement and Interpretation of Fermion-Pair Production at LEP energies from 130 to 172 GeV*" Eur. Phys. J. **C11** (1999), 383;  
DELPHI Collab., "*Measurement and Interpretation of Fermion-Pair Production at LEP Energies from 183 to 189 GeV*" Phys.Lett. **B485** (2000), 45;  
DELPHI Collab., "*Results on Fermion-Pair Production at LEP running from 192 to 202 GeV*" DELPHI 2000-128 OSAKA CONF 427 (2000);  
L3 Collab., "*Measurement of Hadron and Lepton-Pair Production at  $161 \text{ GeV} < \sqrt{s} < 172 \text{ GeV}$  at LEP*" Phys. Lett. B 407 (1997) 361;  
L3 Collab., "*Measurement of Hadron and Lepton-Pair Production at  $130 \text{ GeV} < \sqrt{s} < 189 \text{ GeV}$  at LEP*", Phys. Lett. **B479** (2000), 101.  
L3 Collab., "*Preliminary L3 Results on Fermion-Pair Production in 1999*", L3 note 2563;  
OPAL Collab., "*Tests of the Standard Model and Constraints on New Physics from Measurements of Fermion Pair Production at 130 - 172 GeV at LEP*", Euro. Phys. J. **C2** (1998) 441;  
OPAL Collab., "*Tests of the Standard Model and Constraints on New Physics from Measurements of Fermion Pair Production at 183 GeV at LEP*", Euro. Phys. J. **C6** (1999) 1;  
OPAL Collab., "*Tests of the Standard Model and Constraints on New Physics from Measurements of Fermion Pair Production at 189 GeV at LEP*", Euro. Phys. J. **C13** (2000) 553;  
OPAL Collab., "*Tests of the Standard Model and Constraints on New Physics from Measurements of Fermion Pair Production at 192-202 GeV at LEP*", OPAL PN424 (2000).
- [5] D. Bardin *et al.*, CERN-TH 6443/92; <http://www.ifh.de/~riemann/Zfitter/zf.html> .  
Definition 1 corresponds to the ZFITTER flags FINR=0 and INTF=0; definition 2 corresponds to FINR=0 and INTF=1 for hadrons, FINR=1 and INTF=1 for leptons.
- [6] G. Montagna *et al.*, Comput. Phys. Commun. **117** (1999) 278;  
<http://www.to.infn.it/~giampier/topaz0.html> .
- [7] S. Jadach *et al.*, <http://home.cern.ch/~jadach/KKindex.html> .
- [8] The error quoted is slightly larger than that given in the *Report of the LEP II Monte Carlo Workshop*, M. Kobel *et al.*, "*Two-Fermion Production in Electron Positron Collisions*", hep-ph/0007180.
- [9] ALEPH Collaboration, Euro. Phys J. **C12** (2000) 183;  
DELPHI Collaboration, P.Abreu *et al.*, Euro. Phys J. **C11**(1999);  
L3 Collaboration, M.Acciarri *et al.*, Phys. Lett. **B485** (2000) 71;  
OPAL Collaboration, G.Abbiendi *et al.*, Euro. Phys. J. **C16** (2000) 41.

- [10] ALEPH Collaboration, ALEPH 99-018 CONF 99-013;  
ALEPH Collaboration, ALEPH 2000-046 CONF 2000-029;  
DELPHI Collaboration, DELPHI 2000-129 CONF 428;  
L3 Collaboration, L3 Internal note 2538, 16 May 2000;  
L3 Collaboration, L3 Internal note 2556, 30 June 2000.
- [11] LEPEWWG Heavy Flavour at LEP2 Subgroup, "Combination of Heavy Flavour Measurements at LEP2", LEP2FF/00-02.
- [12] ZFITTER V6.23 is used.  
D. Bardin *et al.*, Preprint hep-ph/9908433.  
Relevant ZFITTER settings used are FINR=0 and INTF=1.
- [13] The LEP Experiments: ALEPH, DELPHI, L3 and OPAL, Nucl. Inst. Meth. **A378** (1998) 101.
- [14] DELPHI Collaboration, P. Abreu *et al.*, Euro Phys J. **C10**(1999) 415.  
The LEP collaborations *et al.*, CERN-EP/2000-016.
- [15] P. Langacker, R.W. Robinett and J.L. Rosner, Phys. Rev. **D30** (1984) 1470;  
D. London and J.L. Rosner, Phys. Rev. **D34** (1986) 1530;  
J.C. Pati and A. Salam, Phys. Rev. **D10** (1974) 275;  
R.N. Mohapatra and J.C. Pati, Phys. Rev. **D11** (1975) 566.
- [16] G. Altarelli *et al.*, Z. Phys. **C45** (1989) 109;  
erratum Z. Phys. **C47** (1990) 676.
- [17] DELPHI Collab., P. Abreu *et al.*, Zeit. Phys. **C65** (1995) 603
- [18] E. Eichten, K. Lane and M. Peskin, Phys. Rev. Lett. **50** (1983) 811.
- [19] H. Kroha, Phys. Rev. **D46** (1992) 58.
- [20] A. Leike, T. Riemann, and J. Rose, Phys. Lett. **B 273** (1991) 513;  
T. Riemann, Phys. Lett. **B 293** (1992) 451;  
S. Kirsch, T. Riemann, Comp. Phys. Comm. **88** (1995) 89.
- [21] The 4 LEP experiments : ALEPH, DELPHI, L3 and OPAL, the LEP Electroweak Working Group, and the SLD Heavy Flavour and Electroweak Groups, "*A Combination of Preliminary Electroweak Measurements and Constraints on the Standard Model*", CERN-EP/99-015 (1999).
- [22] The 4 LEP experiments : ALEPH, DELPHI, L3 and OPAL, the LEP Electroweak Working Group, and the SLD Heavy Flavour and Electroweak Groups, "*A Combination of Preliminary Electroweak Measurements and Constraints on the Standard Model*", Note in preparation, summer 2000.
- [23] S. Kirsch and T. Riemann, "*SMATASY – A program for the model independent description of the Z resonance*", DESY 94-125 (1994).  
SMATASY version 6.23 is used together with ZFITTER version 6.23.